Inorg. Chem. **2006**, *45*, 1208–1214

Synthesis of Variable-Aspect-Ratio, Single-Crystalline ZnO Nanostructures

Bin Cheng,[†] Wensheng Shi,[†] Joette M. Russell-Tanner,[†] Lei Zhang,[‡] and Edward T. Samulski*[,†,‡]

Department of Chemistry and Curriculum in Applied Materials Sciences, University of North Carolina, Chapel Hill, North Carolina 27599-3290

Received October 15, 2005

Variable-aspect-ratio (length/diameter), one-dimensional (1-D) ZnO nanostructures (nanorods and nanowires) were prepared in alcohol/water solution by reacting a Zn^{2+} precursor with an organic weak base, tetramethylammonium hydroxide (Me_4NOH). The effect of the experimental parameters (temperature, base concentration, reaction time, and water content) on nucleation, growth, and the final morphology of the ZnO nanostructures was investigated. The low-temperature syntheses (75–150 °C) yielded aspect ratios of the 1-D ZnO nanostructures that depended on the water content. The individual ZnO nanorods and nanowires were determined to be perfect, single crystals with their *c* axes as the primary growth direction.

Introduction

The wide-band-gap II−IV semiconductor ZnO is structurally isomorphous and exhibits a polarity identical to that of the III−V semiconductor GaN. Due to the ease of synthesis of oxides relative to nitrides, ZnO is increasingly viewed as an attractive alternative to GaN.[1,2] One-dimensional (1-D) ZnO nanostructures have application in optoelectronic nanoscale devices such as nanolasers,[3] gas sensors,[4] transistors,[5] and nanoresonators.[6] Many synthetic methodologies for 1-D ZnO nanostructrures have been developed, including "dry" methods (e. g., thermal evaporation,[7] chemical vapor deposition,[8] metal−organic chemical vapor deposition,[9] molecular beam epitaxy,[10] and template-base methods[11]) and "wet" solution-phase methods.[12] The synthesis of 1-D ZnO nanostructures via the latter route includes microemulsion techniques,[13] direct growth in aqueous-alcohol solution,[14] and surfactant-assisted growth.[15] The "dry" methods employ high temperature and complicated equipment in contrast with the lower-cost and facile "wet" processes. Herein, we investigate the fundamental nucleation and growth of ZnO nanostructures in alcohol/water media having high pH by introducing a weak organic base—tetramethylammonium hydroxide (Me_4NOH). Variable-aspect-ratio, 1-D ZnO nanostructures (nanorods and nanowires) were obtained under mild conditions from the reaction of a Zn^{2+} precursor with Me_4NOH. The advantage of our method over other wet chemical routes to ZnO nanoparticles is that we can directly control the nanoparticle's aspect ratio by merely specifying the water content in the reaction media.

Experimental Section

$Zn(Ac)_2 \cdot 2H_2O$ (Aldirch), $Zn(NO_3)_2 \cdot 6H_2O$ (Aldrich), $ZnCl_2 \cdot xH_2O$ (Alfa Aesar), Me_4NOH (25% w/w in methanol) (Alfa Aesar), Me_4NOH (25% w/w in water) (Alfa Aesar). All of the above materials were used without further purification.

* To whom correspondence should be addressed. E-mail: et@unc.edu.
† Department of Chemistry.
‡ Curriculum in Applied Materials Sciences.

(1) Look, D. C.; Hemsky, J. W.; Sizelove, J. R. *Phys. Rev. Lett.* **1999**, *82*, 2552.
(2) Tuomisto, F.; Ranki, V.; Saarinen, K.; Look, D. C. *Phys. Rev. Lett.* **2003**, *91*, 205502.
(3) Huang, M.; Mao, S.; Feick, H.; Yan, H.; Wu, Y.; Kind, H.; Weber, E.; Russo, R.; Yang, P. *Science* **2001**, *292*, 1897.
(4) Comini, E.; Faglia, G.; Sberveglier, G.; Pan, Z.; Wang, Z. L. *Appl. Phys. Lett.* **2002**, *81*, 1869.
(5) Arnold, M. S.; Avouris, P.; Pan, Z. W.; Wang, Z. L. *J. Phys. Chem. B* **2003**, *107*, 659.
(6) Shi, L.; Hao, Q.; Yu, C.; Mingo, N.; Kong, X.; Wang, Z. L. *Appl. Phys. Lett.* **2004**, *84*, 2638.
(7) Pan, Z. W.; Dai, Z. R.; Wang, Z. L. *Science* **2001**, *291*, 1947.
(8) Wu, J. J.; Liu, S. C. *Adv. Mater.* **2002**, *14*, 215.
(9) Zhang, B. P.; Binh, N. T.; Segawa, Y.; Wakatsuhi, K.; Usami, N. *Appl. Phys. Lett.* **2003**, *83*, 1638.
(10) Heo, Y. W.; Varadarajan, V.; Kaufman, M.; Kim, K.; Norton, D. P.; Ren, F.; Fleming, P. H. *Appl. Phys. Lett.* **2002**, *81*, 3046.
(11) Li, Y.; Meng, G. W.; Zhang, L. D.; Phillipp, F. *Appl. Phys. Lett.* **2000**, *76*, 2011.
(12) (a) Liu, B.; Zeng, H. C. *J. Am. Chem. Soc.* **2003**, *125*, 4430. (b) Tian, Z.; Voigt, J. A.; Liu, J.; Mckenzie, B.; Mcdermott, M. J.; Rodriguez, M. A.; Konishi, H.; Xu, H. *Nat. Mater.* **2003**, *2*, 821.
(13) Guo, L.; Ji, Y. L.; Xu, H.; Simon, P.; Wu, Z. *J. Am. Chem. Soc.* **2002**, *124*, 14864.
(14) Pacholski, C.; Kornowski, A.; Weller, H. *Angew. Chem., Int. Ed.* **2002**, *41*, 1188.
(15) Zhang, H.; Yang, D.; Ji, Y.; Ma, X.; Xu, J.; Que, D. *J. Phys. Chem. B* **2004**, *108*, 3955.

10.1021/ic051786a CCC: $33.50
Published on Web 01/06/2006

1. ZnO Nanostructure Growth under Constant Water Content Conditions. The Zn^{2+} precursor ($Zn(Ac)_2 \cdot 2H_2O$, 0.005 mol) was dissolved in 10 mL of methanol, after which 20 mL of the commercial base Me_4NOH (25% w/w in methanol) was added with stirring at room temperature. The solution was transferred to a Teflon-lined stainless steel autoclave and heated at a selective temperature for specific times. The reaction was terminated and cooled to room temperature. A white precipitate was collected by centrifugation and purified by washing with water several times. Several important parameters (reaction temperature, concentration of Me_4NOH, and reaction time) were varied in order to investigate their effect on the ZnO growth and its final morphology.

2. ZnO Nanostructure Growth under Variable Water Content Conditions. 2.1. Synthesis of Short ZnO Nanorods (Low Water Content). $Zn(Ac)_2 \cdot 2H_2O$ was dissolved in 10 mL of methanol to give 0.005 mol of Zn^{2+} precursor. Then, 20 mL of the commercial base Me_4NOH (25% w/w in methanol) was added with stirring at room temperature. The solution was transferred to a Teflon-lined stainless steel autoclave and heated at 75 °C for 24 h. The white precipitate was collected and purified by washing with water and dried in air at room temperature.

2.2. Synthesis of Long ZnO Nanorods (Intermediate Water Content). A 10 mL methanol stock solution was prepared with 0.005 mol of Zn^{2+} ion precursor by dissolving $Zn(Ac)_2 \cdot 2H_2O$ or other Zn^{2+} compounds. Separately, 5 mL of Me_4NOH (25% w/w in water) was mixed with 15 mL of Me_4NOH (25% w/w in methanol) to generate a basic solution which was added to the Zn^{2+} stock solution under stirring at room temperature. The reaction mixture was transferred to a Teflon-lined stainless steel autoclave and heated at 75 °C for 24 h. The white precipitate was collected and purified by washing with water and then dried in air at room temperature.

2.3. Synthesis of ZnO Nanowires (High Water Content). Fifteen milliliters of Me_4NOH (25% w/w in water) mixed with 5 mL of Me_4NOH (25% w/w in methanol) basic solution was added to the 0.005 mol Zn^{2+} stock solution with stirring at room temperature. The solution was transferred to a Teflon-lined stainless steel autoclave and heated at 75 °C for 24 h. The white precipitate was collected and purified by washing with water and dried in air at room temperature.

Characterization. The synthesized products were characterized by X-ray powder diffraction (XRD, Rigaku Multiflex X-ray diffractometer, with Cu Kα radiation, $\lambda = 0.154178$ nm at 40 kV and 40 mA), transmission electron microscopy (TEM; Philips CM-12, with a accelerating voltage of 100 kV), and high-resolution transmission electron microscopy (HRTEM; Topcon EM-002B, with a accelerating voltage of 200 kV). Photoluminescence measurements were conducted using a He−Cd laser (Melles Griot, Model 2056) with unpolarized 12 mW output at 325 nm as the excitation light.

Results and Discussion

To understand the nucleation and growth of ZnO nanostructures in methanol/water mixtures with the weak organic base Me_4NOH, several important synthetic parameters (reaction temperature, base concentration, reaction time, methanol/water ratio, etc.) were investigated. Figure 1 shows the effect of reaction temperature on the morphology of the resulting ZnO nanostructures at low water content (0.06% H_2O). Figure 1A shows the TEM image of the ZnO nanostructures prepared at 50 °C for 24 h. All of the product is comprised of quasi-spherical nanoparticles with an average diameter of 10 nm. Figure 1B shows the result of the reaction at 50 °C for 48 h. The morphology is still quasi-spherical nanoparticles, the same as that in Figure 1A. After the solution was heated at 50 °C for 24 h, the temperature was then elevated to 150 °C for another 24 h. Almost all of the final product is comprised of nanorods with an average length of 50 nm and average diameter of 15 nm (Figure 1C) with a few coexisting quasi-spherical nanoparticles. The diameter of the ZnO nanorods is larger than the diameter of the nanoparticles shown in Figure 1A and B. Temperature proved to be critical to the formation of ZnO nanorods at low water content. Anisotropic growth to form nanorods only happened at relatively high temperatures (>50 °C).

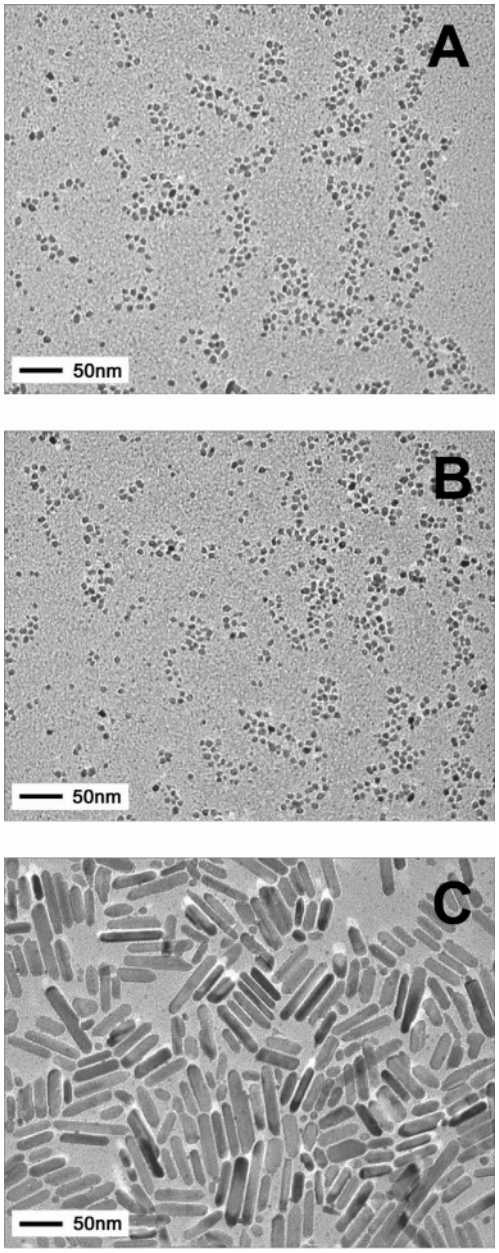

Figure 1. TEM images of the low-water-content product of ZnO nanostructure prepared under different thermal histories. (A) 50 °C for 24 h; (B) 50 °C for 48 h; (C) 50 °C for 24 h followed by a period at elevated temperature 150 °C for another 24 h.

The concentration of Me_4NOH was also varied to investigate its effect on the morphology of ZnO. The reaction of

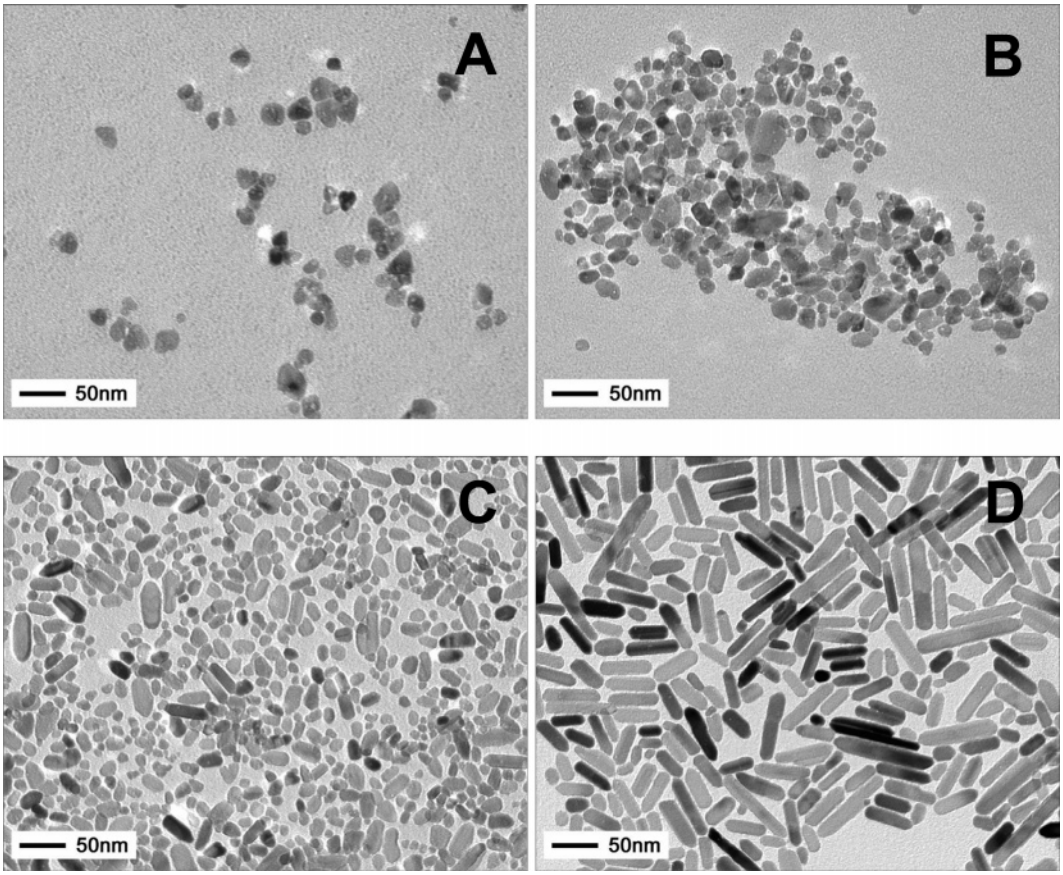

Figure 2. TEM images of the ZnO nanostructures prepared with different concentrations of Me_4NOH at low water content (0.06%): (A) 6% Me_4NOH (v/v), (B) 16% Me_4NOH (v/v), (C) 32% Me_4NOH (v/v), and (D) 66% Me_4NOH (v/v). The precursor Zn^{2+} concentration (0.16 mol/L), temperature (150 °C), and reaction time (24 h) were kept constant.

Zn^{2+} precursors with OH^- ions has been thoroughly studied.[16] When the molar ratio of Zn^{2+} to OH^- is higher, the initial reaction mixture is clear and may be represented by the reaction equations:

$$Zn^{2+} + 4OH^- \rightarrow [Zn(OH)_4]^{2-} \quad (1)$$

$$[Zn(OH)_4]^{2-} \rightarrow ZnO_2^{2-} + 2H_2O \quad (2)$$

The ZnO_2^{2-} ions were proposed to be responsible for the polar growth of ZnO under hydrothermal conditions.[18] According to eqs 1 and 2, the concentration of ZnO_2^{2-} increases with increasing OH^- concentration. Figure 2 shows the effect of Me_4NOH concentration on the morphology of the ZnO nanostructures prepared at low water (0.06%) content. Figure 2A shows irregular ZnO nanoparticles prepared at 150 °C for 24 h with a Me_4NOH concentration of 6% (v/v). Figure 2B shows the TEM image of the ZnO particles prepared with a Me_4NOH concentration of 16% (v/v). When the concentration of the Me_4NOH was increased to 33% (v/v), quasi-spherical nanoparticles and short nanorods of ZnO coexisted (Figure 2C). Figure 2D shows that almost all of the product is comprised of the ZnO nanorods with the highest concentration (66% v/v) of Me_4NOH. This experimental result indicates that when the water content was kept low (0.06%), the formation of ZnO nanorods only happens at high concentrations of Me_4NOH. The concentration of ZnO_2^{2-} is proportional to the $[OH^-]$ (see eqs 1 and 2). The high concentration of the "polar growth unit," the "ZnO_2^{2-}" ion, should lead to fast, anisotropic growth of ZnO along the *c* axis, the [0001] direction; see Figure 2D.

Figure 3 shows the different morphologies of ZnO nanostructures prepared at different reaction times at constant Zn^{2+} concentration, Me_4NOH concentration, reaction temperature, and water content (0.005 mol, 66% v/v, 150 °C and 0.06%, respectively). Figure 3A−F shows the corresponding morphologies of ZnO nanostructures resulting from varying the reaction time from 4 to 24 h. For a reaction time of 4 h, Figure 3A shows the coexistence of short nanorods and quasi-spherical morphologies. When the reaction time was doubled to 8 h (Figure 3B, the morphology is 1ess quasi-spherical and more rodlike. The morphology was almost completely changed to nanorods when the reaction was conducted for 24 h (see Figure 3F). Longer and wider ZnO nanorods preferentially grow with the dissolution of smaller, quasi-spherical nanoparticles (Ostwald ripening).

Figure 4 shows the TEM images of 1-D ZnO nanostructures (nanorods and nanowires) with different aspect ratios (L/D) which were synthesized from the variable-water-content system. Low water content (0.06%) would lead to formation of short ZnO nanorods with average length of 48 nm and diameter of 15 nm (Figure 4A). When the water

(16) (a) Liu, B.; Zeng, H. C. *Langmuir* **2004**, *20*, 4196. (b) Li, W.-J.; Shi, E.-W.; Zhong, W.-Z.; Yin, Z.-W. *J. Cryst. Growth* **1999**, *203*, 186.

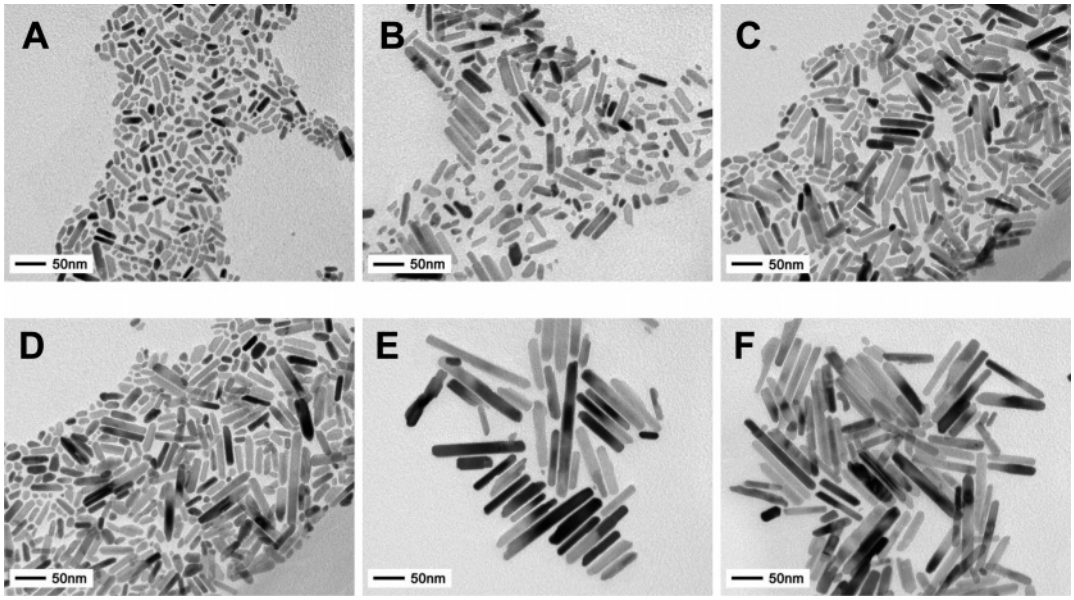

Figure 3. TEM images of the ZnO nanostructures prepared at different reaction times: (A) 4, (B) 8, (C) 12, (D) 16, (E) 20, and (F) 24 h. The precursor Zn^{2+} concentration (0.16 mol/L), Me_4NOH concentration (66%, v/v), temperature (150 °C), and water content (0.06%) were kept constant.

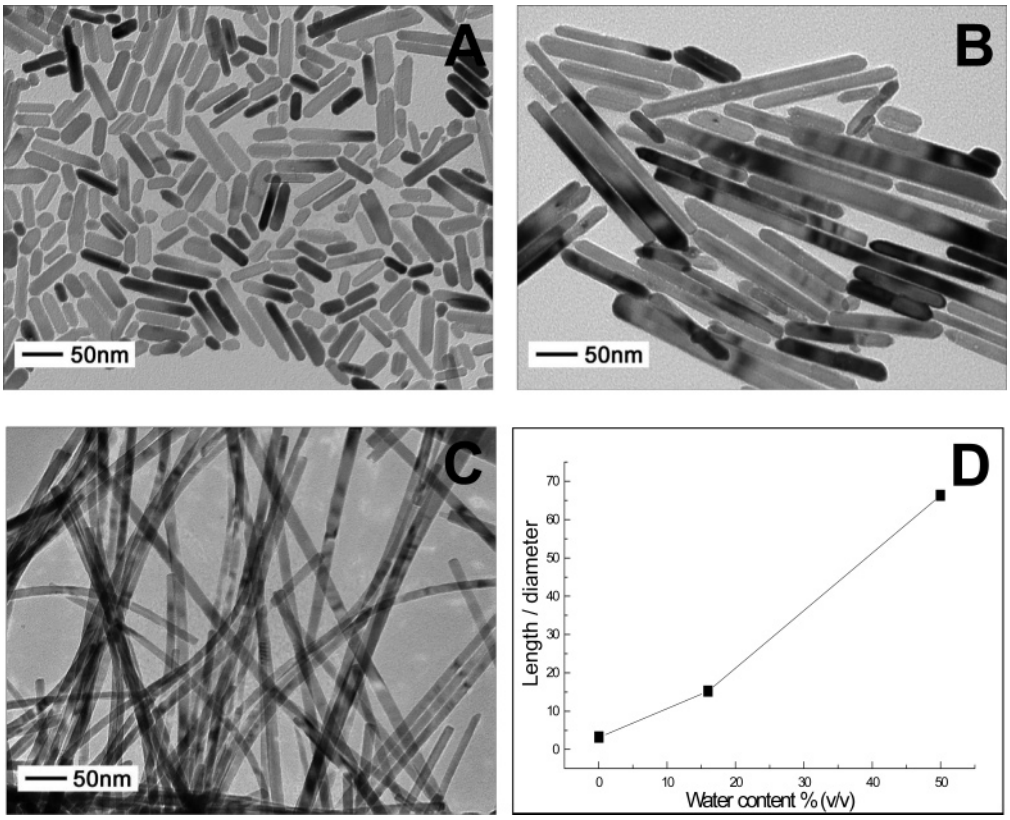

Figure 4. TEM images of the as-prepared 1-D ZnO nanostructures with different L/D, aspect ratios (length/diameter); (A) nanorods with L/D = 4:1; (B) nanorods with L/D = 10:1; (C) nanowires with L/D = 50:1; (D) average aspect ratio of the 1-D ZnO nanostructures as function of water content in the reaction system.

content was increased to 16% (v/v), the dimensions of the ZnO nanorods were changed with average length of 370 nm and diameter of 20 nm (see Figure 4B). Figure 4C shows the TEM image of the as-prepared ZnO nanowires with average length of 1087 nm and diameter of 17 nm prepared with a 50% water content. The average L/D of the 1-D ZnO nanorods and nanowires as a function of water content is shown in Figure 4D.

The 1-D preferred growth along the ZnO *c* axis under hydrothermal conditions appears to be related to its intrinsic crystal structure and external factors.[16,17] After nucleation, the particles grow by diffusion of reactant units to the surfaces of the particles. ZnO is a typical polar crystal, and the "polar growth unit" ZnO_2^{2-} adds to both the positive

(17) Cheng, B.; Samulski, E. T. *Chem. Commun.* **2004**, 986.

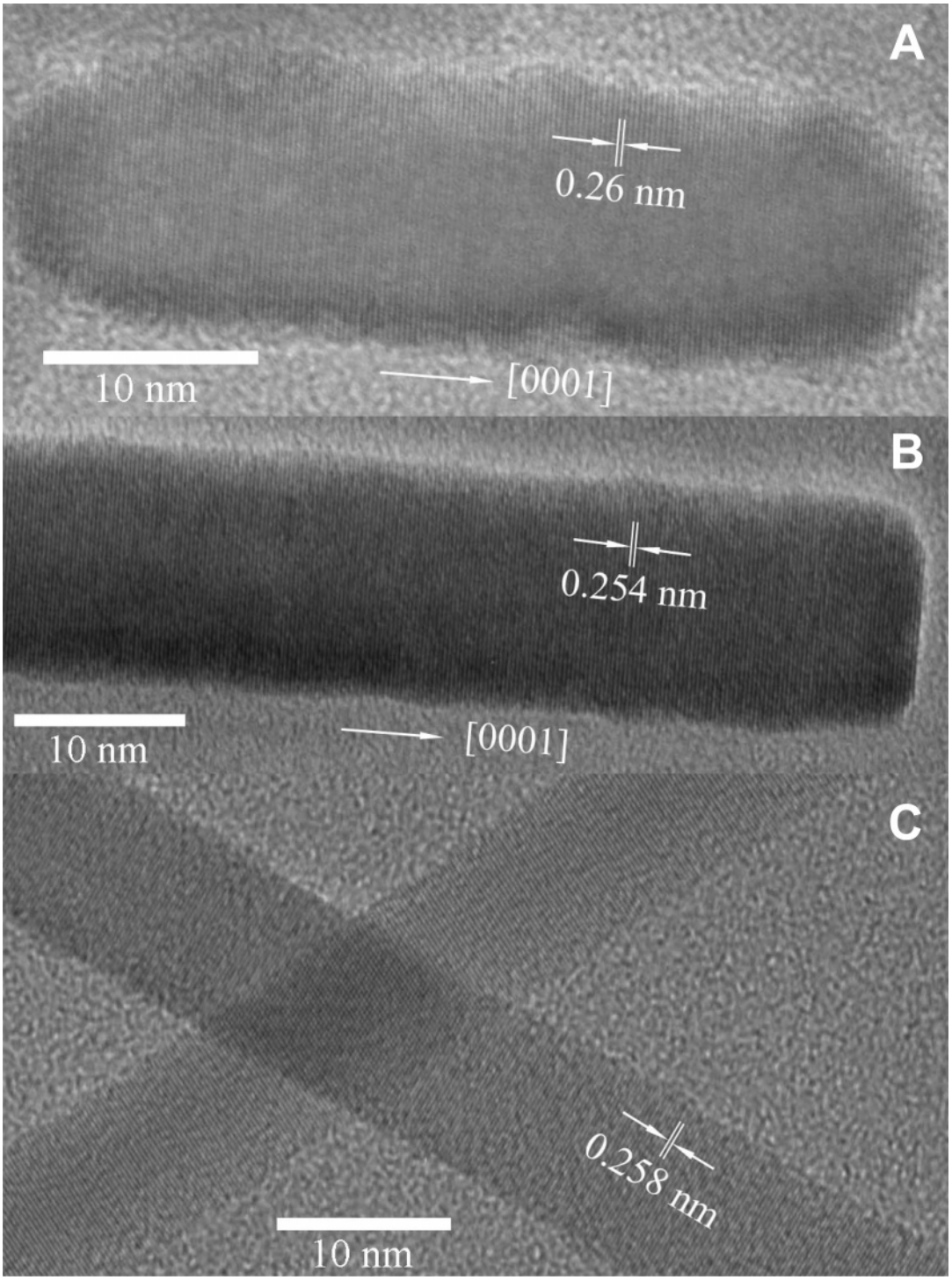

Figure 5. High-resolution transmission electron microscopy (HRTEM) images of 1-D ZnO nanostructures (prepared in solution at 75 °C) with different aspect ratios: (A) a short individual ZnO nanorod with a mean L/D = 4:1, (B) one end of an individual ZnO intermediate-size nanorod with L/D = 10:1, and (C) two overlapping ZnO nanowires with L/D = 50:1.

(0001) and negative (000−1) monohedron faces.[18] The number of nuclei for a fixed Zn^{2+} ion concentration—the stoichiometry—determines the ultimate length of the nanorods. However, nuclei formation and growth is complex: there is a dynamic balance between temperature-sensitive processes such as the dissociation of a weak base (which enables the nucleation of ZnO), the rate of growth of those nuclei, and their concomitant dissolution (Ostwald ripening). When the water content is low (0.06%), very few nuclei are formed during the mixing of the Zn^{2+} salt and the weak Me_4-NOH base at room temperature because the concentration of OH^- ions is very low. Elevating the temperature (to 75 °C) shifts the dissociation of the weak base, and the concentration of OH^- ions precipitously increases. While the

(18) Demyanets, L. N.; Kostomarov, D. V.; Kuzmina, I. P. *Inorg. Mater.* **2002**, *38*, 124.

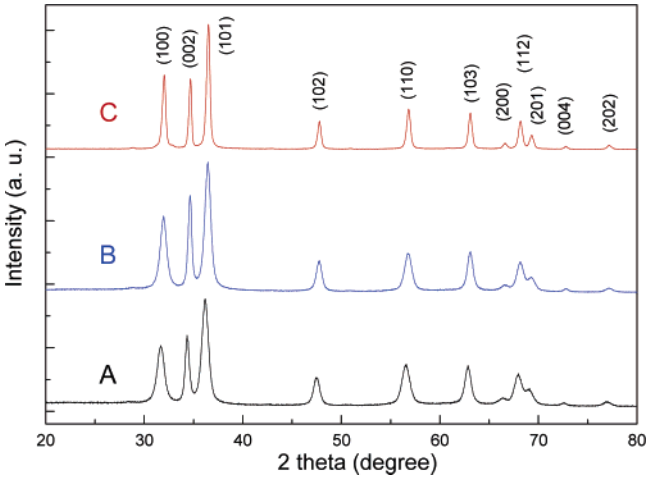

Figure 6. X-ray diffraction patterns of the as-prepared 1-D ZnO nanostructures with different aspect ratios: (A) L/D = 4:1, (B) L/D = 10:1, and (C) L/D = 50:1.

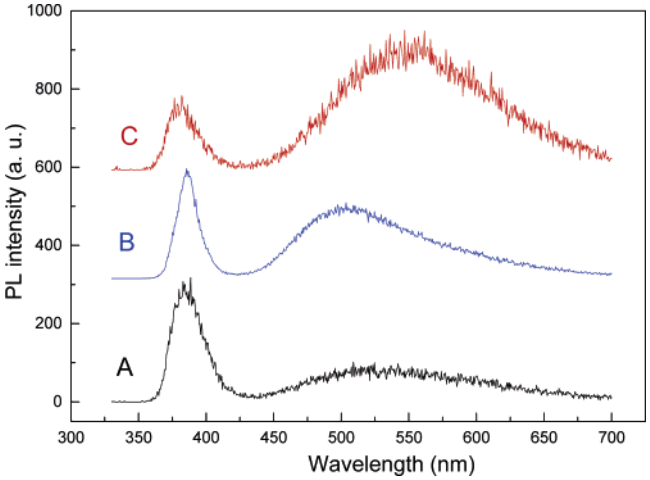

Figure 7. Room-temperature photoluminescence spectra of the as-prepared 1-D ZnO nanostructures with different aspect ratios: (A) L/D = 4:1, (B) L/D = 10:1, and (C) L/D = 50:1.

growth rate of nuclei increases when the temperature is raised, the growth of the initially formed nuclei is overwhelmed by the production of many more nuclei when the low-water-content solution is heated and the OH^- ion concentration increases. As a result, a distribution of short nanorods is produced under these conditions (see Figure 4A). By contrast, syntheses having increased amounts of water are dominated by those nuclei that are formed during the mixing stage at room temperature; raising the temperature primarily increases the growth rate of those relatively few nuclei. As a result, high-aspect-ratio nanorods and nanowires predominate in the high-water-content reactions.

The single-crystalline structural details of the 1-D ZnO nanostructures were characterized by HRTEM. Figure 5 shows the HRTEM images of the 1-D ZnO nanostructures with different aspect ratios. Figure 5A shows a short individual ZnO nanorod with a mean L/D = 4:1. Figure 5B shows one end of an individual ZnO intermediate size nanorod with L/D = 10:1. Figure 5C shows two overlapping ZnO nanowires with L/D = 50:1. The HRTEM images indicate that all three aspect-ratio nanostructures are single-crystalline. Moreover, there does not appear to be any significant amorphous ZnO or defects on the exterior of the nanorods and nanowires. The HRTEM results show that the 1-D ZnO grows along its [0001] direction; the lattice spacing (2.54 ± 0.05 Å) corresponds to the distance between two (0001) planes. Each individual ZnO nanorod or nanwire is a perfect single crystal with its *c* axis as the growth direction. Figure 6 shows the corresponding XRD patterns. All three XRD patterns can be indexed as the hexagonal wurtzite structure of ZnO with respective lattice constant sets $\{a_A = 3.254$ Å, $c_A = 5.211$ Å$\}$, $\{a_B = 3.243$ Å, $c_B = 5.193$ Å$\}$, and $\{a_C = 3.241$ Å, $c_C = 5.193$ Å$\}$ that are in good agreement with the JCPDS file of ZnO (JCPDS 36-1451).

The photoluminescence from ZnO consists of two emission bands at room temperature: a near-band-edge (UV) light emission, and a broad, deep-level (visible) emission.[22,23] The visible emission is usually considered to be related to various intrinsic defects produced during ZnO preparation and post-treatment.[24,25] Normally, these defects are located at the surface of the ZnO structure.[24−26] Figure 7 shows the room-temperature photoluminescence spectra of 1-D ZnO nanostructures measured using a He−Cd laser (325 nm) as an excitation source. All three aspect ratios show a strong UV emission around 384 nm and a broad visible emission between 500 and 550 nm, respectively. The UV emission is the band-edge emission resulting from the recombination of excitonic centers.[19] The green emission at ~525 nm in Figure 7 results from the recombination of electrons in singly occupied oxygen vacancies with photoexcited holes.[20] The luminescence at 550 nm is likely from deep-level sources, e.g., interstitial oxygen.[21] Generally, the overall shape of the visible emission is a function of defects which in turn, vary from sample to sample. It is desirable to have the intensity of the visible emission to be as low as possible for many applications. Hence, the intensity of the visible ratio of the UV to the visible emission is usually employed as an important criterion to indirectly evaluate the quality of ZnO.[27−31] However, we recently found not only that the

(19) Huang, M. H.; Wu, Y. Y.; Feick, H. N.; Tran, N.; Weber, E.; Yang, P. D. *Adv. Mater.* **2001**, *13*, 113.
(20) (a) Vanheusden, K.; Warren, W. L.; Seager, C. H.; Tallant, D. R.; Voigt, J. A.; Gnade, B. E. *J. Appl. Phys.* **1996**, *79*, 7983. (b) van Dijken, A.; Meulenkamp, E. A.; Vanmaekelbergh, D.; Meijerink, A. *J. Lumin.* **2000**, *90*, 123.
(21) (a) Liu, M.; Kitai, A. H.; Mascher, P. *J. Lumin.* **1992**, *54*, 35. (b) Greene, L. E.; Law, M.; Goldberger, J.; Kim, F.; Johnson, J. C.; Zhang, Y.; Saykally, R. J.; Yang, P. *Angew. Chem., Int. Ed.* **2003**, *42*, 3031.
(22) Fonoberov, V. A.; Balandin, A. A. *Appl. Phys. Lett.* **2004**, *85*, 5971.
(23) Lim, J. M.; Shin, K. C.; Kim, H. W.; Lee, C. M. *J. Lumin.* **2004**, *109*, 181.
(24) Hsu, N. E.; Hung, W. K.; Chen, Y. F. *J. Appl Phys.* **2004**, *96*, 4671.
(25) Li, D.; Leung, Y. H.; Djurisic, A. B.; Liu, Z. T.; Xie, M. H.; Shi, S. L.; Xu, S. J.; Chan, W. K. *Appl. Phys. Lett.* **2004**, *85*, 1601.
(26) Shalish, I.; Temkin, H.; Narayanamurti, V. *Phys. Rev. B* **2004**, *69*, 245401.
(27) Park, W. I.; An, S.-J.; Yi, Gyu-Chul Jang, Hyun M. *J. Mater. Res.* **2001**, *16*, 1358.
(28) Wang, J. Z.; Du, G. T.; Zhang, Y. T.; Zhao, B. J.; Yang, X. T.; Liu, D. L. *J. Cryst. Growth* **2004**, *263*, 269.
(29) Djurisic, A. B.; Choy, W. C. H.; Roy, V. A. L.; Leung, Y. H.; Kwong, C. Y.; Cheah, K. W.; Rao, T. K. G.; Chan, W. K.; Lui, H. T.; Surya, C. *Adv. Func. Mater.* **2004**, *14*, 856.

intensity ratio of the UV to visible emissions relied on the sample properties (such as the nanoparticle dimension, morphology, specific surface area, etc.) but that it was also very sensitive to the experimental conditions (such as excitation density, radiation area, etc.).[32] Therefore, the UV-to-visible ratio should not be used exclusively to evaluate the quality of the ZnO.

Concluding Remarks

The growth of ZnO nanostructures in alcohol/water solution in the presence of the weak, organic base Me_4NOH has been investigated. The formation of anisotropic, 1-D ZnO nanostructures under different reaction conditions was found to be highly temperature dependent. The aspect ratio of the 1-D ZnO nanostructures depends not only on reaction time but also on the water content in reaction system. The ratio of alcohol/water was found to be critical to the L/D of the final 1-D ZnO nanostructures. Low water content resulted in short ZnO nanorods (with L/D = 4:1). High water content generated the long ZnO nanorods (with L/D = 10:1) and further to the formation of the ZnO nanowires (with L/D = 50:1) under more water content condition. The use of Me_4NOH not only allowed for high pH reaction conditions but also provided a means for varying the OH^- concentration on the basis of the chemical equilibrium between this base and the water in the reaction system. The control of the aspect ratio of the ZnO nanostructures in solution was realized for the first time by introducing the organic base Me_4NOH and tuning the water content. Moreover, the 1-D ZnO nanostructures (nanorods or nanowires) are perfect single crystals with their *c* axes as the growth directions, and they exhibit characteristic photoluminescence.

Acknowledgment. This work is supported by the NASA University Research, Engineering and Technology Institute on Bio Inspired Materials (BIMat) under award No. NCC-1-02037.

IC051786A

(30) Kim, J.; Shin, K.; Kim, H. W.; Lee, C. *Mater. Sci., Eng. B* **2004**, *107*, 301.
(31) Roy, V. A. L.; Djurisic, A. B.; Chan, W. K.; Gao, J.; Lui, H. F.; Surya, C. *Appl. Phys. Lett.* **2003**, *83*, 141.
(32) Shi, W.; Cheng, B.; Zhang, L.; Samulski, E. T. *J. Appl. Phys.* **2005**, *98*, 083502.